Nat. Hazards Earth Syst. Sci. Discuss., 1, 5237–5260, 2013
www.nat-hazards-earth-syst-sci-discuss.net/1/5237/2013/
doi:10.5194/nhessd-1-5237-2013

Natural Hazards and Earth System Sciences
Open Access
Discussions

Modulational instability and rogue waves in finite water depth

L. Fernandez[1], M. Onorato[2,3], J. Monbaliu[1], and A. Toffoli[4,5]

[1]Department of Civil Engineering, KU Leuven, Kasteelpark Arenberg 40, P.O. Box 2448, 3001 Leuven, Belgium
[2]Dipartimento di Fisica, Università di Torino, Via P. Giuria, Torino, 10125, Italy
[3]INFN, Sezione di Torino, Via Pietro Giuria 1, 10125 Torino, Italy
[4]Centre for Ocean Engineering Science and Technology, Swinburne University of Technology, P.O. Box 218, Hawthorn, VIC., 3122, Australia
[5]School of Marine Science and Engineering, Plymouth University, Plymouth, PL4 8AA, UK

Received: 15 August 2013 – Accepted: 3 September 2013 – Published: 2 October 2013

Correspondence to: A. Toffoli (toffoli.alessandro@gmail.com)

Published by Copernicus Publications on behalf of the European Geosciences Union.

Abstract

The mechanism of side band perturbations to a uniform wave train is known to produce modulational instability and in deep water conditions it is accepted as a plausible cause for rogue wave formation. In a condition of finite water depth, however, the interaction with the sea floor generates a wave-induced current that subtracts energy from the wave field and consequently attenuates this instability mechanism. As a result, a plane wave remains stable under the influence of collinear side bands for relative water depths $kh \leq 1.36$ (where k represents the wavenumber of the plane wave and h the water depth), but it can still destabilise due to oblique perturbations. Using direct numerical simulations of the Euler equations, it is here demonstrated that oblique side bands are capable of triggering modulational instability and eventually leading to the formation of rogue waves also for $kh \leq 1.36$. Results, nonetheless, indicates that modulational instability cannot sustain a substantial wave growth for $kh < 0.8$.

1 Introduction

The occurrence of extreme waves (also known as freak or rogue waves) has an important role in many branches of physics and engineering (see, for example, Chabchoub et al., 2011; Onorato et al., 2013a, b; Chalikov, 2009; Babanin et al., 2011; Bitner-Gregersen and Toffoli, 2012; Toffoli et al., 2008b; Solli et al., 2007; Kibler et al., 2010; Bailung et al., 2011, among many others). Apart from a linear superposition of wave modes and the effect of currents on waves (caustic theory), the modulational instability of a plane wave to side band perturbations remains the most likely mechanism by which rogue waves can appear in deep water (Zakharov and Ostrovsky, 2009; Osborne, 2010; Onorato et al., 2013b; Kharif et al., 2009), i.e. $k_0 h \to \infty$, where k_0 is the wavenumber of the plane wave and h is the water depth. Basically, this is a generalisation of the Benjamin and Feir (1967) or modulational instability (Zakharov, 1968) and can be described by the nonlinear Schrödinger (NLS) equation (Zakharov, 1968), which is derived from the Euler equations by assuming that waves are weakly nonlinear (i.e. the wave steepness $\varepsilon = k_0 a_0 \ll 1$, where a_0 is the amplitude of the plane carrier wave) and the bandwidth in wavenumber space is narrow ($\Delta k / k_0 \ll 1$, where Δk is the modulation wavenumber). For a propagation in one dimension, a linear stability analysis of the NLS equation indicates that unstable disturbances can lead to an exponential growth of a small-amplitude modulation and hence to rogue waves (see, e.g., Osborne, 2010). If two-dimensional propagation is allowed, a 2+1 form of the NLS equation indicates that unstable disturbances are not only limited to the ones propagating collinearly with the plane wave, but also include modes that propagate at an angle with respect to the carrier. Note that the region of instability is stretched over a narrow domain, forming an angle of about 35.5° with the carrier wave direction towards high wavenumbers (see the instability diagram in Fig. 1 of Gramstad and Trulsen, 2011, for example). Although the most unstable modes remain collinear in water of infinite depth, oblique perturbations tend to dominate the modulational instability for condition of arbitrary water depths when $k_0 h < \varepsilon^{-1}$ (Trulsen and Dysthe, 1996). This is also confirmed by laboratory experiments in a relatively wide long wave flume (Trulsen et al., 1999), where a plane wave without any initial seeding of unstable modes was observed to transfer energy towards a lower oblique side band (see also Babanin et al., 2011; Ribal et al., 2013). Direct numerical simulations of the 2+1 NLS equation, furthermore, substantiate that not only can oblique disturbances sustain modulational instability, but they are also capable of triggering the formation of rogue waves (Osborne et al., 2000; Slunyaev et al., 2002). For conditions of more finite water depths, $k_0 h \approx O(1)$, wave-induced mean flow gradually subtracts energy from the wave fields with a concurrent weakening of the modulational instability mechanism (see, e.g., Slunyaev et al., 2002; Benjamin, 1967; Whitham, 1974; Janssen and Onorato, 2007; McLean, 1982; Benney and Roskes, 1969). As a result, there is a reduction of the region of instability (see Fig. 1 in Gramstad and Trulsen, 2011), leading to a complete stabilisation of collinear modes at a critical relative water depths $k_0 h = 1.36$ (Benjamin, 1967; Janssen and Onorato, 2007). Beyond this threshold, nevertheless, oblique perturbations still remain unstable

NHESSD
1, 5237–5260, 2013

Title Page
Abstract Introduction
Conclusions References
Tables Figures
◂ ▸
Back Close
Full Screen / Esc
Printer-friendly Version
Interactive Discussion

and numerical simulations of the 2+1 NLS equation, in this respect, confirm that such modes can still trigger very large amplitude waves (Slunyaev et al., 2002). Moreover, direct numerical simulations of the Euler equation for random finite water depth directional wave fields, show that the formation of extreme waves is sustained, leading to substantial deviations from standard second-order based statistics (Toffoli et al., 2009). A methodical analysis on the effect of oblique perturbations on the nonlinear dynamics of a plane wave has not been attempted yet and hence the transition between infinite and finite depth still remains not completely clear. It is reasonable to expect, moreover, that the region of instability would eventually vanish for sufficiently shallow water depths. Therefore, there should exist a lower limit beyond which wave amplitude growth would cease. In the present paper, the nonlinear evolution of a plane wave in relative water depth gradually varying from deep water ($k_0 h \rightarrow \infty$) to shallow water ($k_0 h \rightarrow 0$) conditions and for different degrees of nonlinearity (i.e. wave steepness) is discussed. The problem is approached numerically by solving the Euler equations for the wave motion with a Higher Order Spectral Method (HSOM) (West et al., 1987; Dommermuth and Yue, 1987). In the next two sections a concise description of the model and how its initial conditions are set is presented. In Section 4, the evolution in time of the wave field is discussed; nonlinear energy transfer between the carrier and the unstable perturbation waves and wave amplitude growth are presented. In the final Section, some concluding remarks are given.

2 The model

Under the hypotesis of an incompressible, inviscid and irrotational fluid flow, a velocity potential $\phi(x,y,z,t)$ that satisfies the Laplace's equation in the whole domain of the fluid can be defined. For the present study, a constant water depth is also assumed. At the bottom ($z = -h$) the vertical velocity is imposed and set to zero ($\phi_z|_{-h} = 0$). The free surface elevation and the velocity potential $\psi(x,y,t) = \phi(x,y,\eta(x,y,t),t)$ satisfy the kinematic and dynamic free surface boundary conditions at $z = \eta(x,y,t)$. This leads to the following two equations in the free surface variables (see, e.g., Zakharov, 1968):

$$\psi_t + g\eta + \frac{1}{2}\left(\psi_x^2 + \psi_y^2\right) - \frac{1}{2}W^2\left(1 + \eta_x^2 + \eta_y^2\right) = 0, \quad (1)$$

$$\eta_t + \psi_x\eta_x + \psi_y\eta_y - W\left(1 + \eta_x^2 + \eta_y^2\right) = 0, \quad (2)$$

where partial derivatives are indicated by subscripts and where the vertical velocity at the free surface is indicated by $W(x,y,t) = \phi_z|_\eta$ The system of Eqs. (1) and (2) can be solved using a higher order spectral method (HOSM) giving as a result the time evolution of the surface elevation. Clarmond et al. (2006) showed that the approach of West et al. (1987) is more consistent than the independently developed approach of Dommermuth and Yue (1987). Therefore the former approach was used in this study. HOSM is based on a pseudo–spectral approach that uses a series expansion in the wave steepness ε of the velocity potential of the form:

$$\phi(x,y,z,t) = \sum_{m=1}^{M} \phi^{(m)}(x,y,z,t), \quad (3)$$

where each $\phi^{(m)}$ is a quantity of order $O(\varepsilon^m)$. In Eq. (3), M represent the order of nonlinearity that is considered. For each term of $\phi^{(m)}$, a Taylor expansion is performed around the point z=0 and combined with the expansion for the potential given by Eq. (3). The following system is obtained after all terms at each order in wave steepness are collected.

$$\begin{aligned}
&\phi^{(1)}(x,y,z=0,t) = \psi(x,y,t);\\
&\phi^{(m)}(x,y,z=0,t) = -\sum_{k=1}^{m-1} \frac{\eta^k}{k!}\frac{\partial^k}{\partial z^k}\phi^{(m-k)}(x,y,z=0,t)
\end{aligned} \quad (4)$$

NHESSD
1, 5237–5260, 2013

for $m = 2, 3, \ldots, M$. following West et al. (1987), $W(x,y,t)$ can in a similar way be expanded in series and collected in order of wave steepness:

$$W(x,y,t) = \sum_{m=1}^{M} W^{(m)}(x,y,t), \tag{5}$$

where the terms $W^{(m)}$ are calculated from the $\phi^{(m)}$ terms:

$$W^{(m)}(x,y,t) = \sum_{k=0}^{m-1} \frac{\eta^k}{k!} \frac{\partial^{k+1}}{\partial z^{k+1}} \phi^{(m-k)}(x,y,z=0,t). \tag{6}$$

Taking a rectangular domain in space with dimensions L_x and L_y in x and y and periodicity in both directions for the wave field, the next expression based on a double Fourier series for each $\phi^{(m)}$ term in finite water depth is used (see, e.g. Dean and Dalrymple, 2000):

$$\phi^{(m)}(x,y,z,t) =$$

$$= \sum_{k,l} c_{k,l}^{(\mathrm{m})} \frac{\cosh\left[k_{k,l}(z+h)\right]}{\cosh\left(k_{k,l}h\right)} cos\left(\omega t - \boldsymbol{k}_{k,l}\cdot\boldsymbol{x}\right), \tag{7}$$

with wavenumbers $k_{k,l} = |\boldsymbol{k}_{k,l}|$ and $\boldsymbol{k}_{k,l} = (k_x, k_y) = \left(\frac{2\pi k}{L_x}, \frac{2\pi l}{L_y}\right)$; $\omega = \sqrt{g|\boldsymbol{k}_{k,l}|}$ is the angular frequency. $c_{k,l}^{(m)}(t)$ represent the time-dependent modal coefficients of the potentials $\phi^{(m)}$. These coefficients are determined from Eq. (4) by using two-dimensional Fast Fourier transform taking the free surface elevation and the free surface velocity potentials as input variables.

In this study, third and fifth-order expansion (i.e. $M = 3$ and 5) are evaluated. It allows the inclusion of four waves interactions (see Tanaka, 2001a, b), which is directly

NHESSD
1, 5237–5260, 2013

responsible for modulational instability. The latter also includes higher order interactions, which are responsible for class-II instability and concurrently for crescent waves (see, for example, McLean, 1982; Kristiansen et al., 2005; Francius and Kharif, 2006).

After evaluating the vertical velocity at the free surface at order M, the free surface velocity potential $\psi(x,y,t)$ and the surface elevation $\eta(x,y,t)$ can be integrated in time from equations (1) and (2). The time integration is then performed by means of a fourth-order Runge–Kutta method with a constant time step. Aliasing errors generated in the nonlinear terms are removed (see West et al., 1987; Tanaka, 2001b, for details). Note, however, that no additional terms were included to take into account wave dissipation. For further details of HOSM, the reader is referred to Tanaka (2001a). The HOSM approach has been applied by several authors to study the nonlinear dynamics of surface gravity waves e.g. Mori and Yasuda (2002), Ducrozet et al. (2007), Toffoli et al. (2008b, a), Toffoli et al. (2009), Toffoli et al. (2010) and Xiao et al. (2013), among others. For examples of other numerical methods the reader is referred to e.g. Annenkov and Shrira (2001), Clamond and Grue (2001) and Zakharov et al. (2002). Clamond et al. (2006) compare the performance of different numerical approaches including HOSM.

3 Initial conditions

The model simulates the temporal evolution of an initial surface $\eta(x,y,t=0)$ and the concurrent velocity potential $\psi(x,y,t=0)$ with periodic boundaries. For the present study, the input surface and potential were defined by superimposing a plane (carrier) wave and four infinitesimal (small-amplitude) unstable side band perturbations. For convenience, we defined the carrier as a monochromatic wave with wavelength $L_0 = 156\,\mathrm{m}$ (wave period $T_0 = 10s$ in deep water) and propagating along the x direction. Several values of wave amplitude were applied to vary the wave steepness and hence the degree of nonlinearity. Overall, wave fields with the following steepness were used: $k_0 a_0 = 0.1$, 0.12 and 0.14, where a_0 is the amplitude of the plane wave. Each configuration was then tested within a wide range of water depths, varying from infinite to

NHESSD
1, 5237–5260, 2013

finite conditions (i.e. $0.5 < k_0 h < \infty$). The four small-amplitude perturbations were carefully selected within the unstable region of the instability diagram and with amplitude equivalent to 0.05 % the one of the carrier wave. The modulational wavenumbers ΔK_x and ΔK_y were defined such that the wave packets contains 5 waves under the modulation along the x directional of propagation and $\Delta K_y/\Delta K_x \approx 0.7$ for $k_0 h > 1.36$ and $\Delta y/\Delta x \approx 0.77$ for $k_0 h < 1.36$. Overall, two lower (i.e. $[-\Delta K_x, \Delta K_y]$, $[-\Delta K_x, -\Delta K_y]$) and two upper (i.e. $[\Delta K_x, \Delta K_y]$, $[-\Delta K_x, -\Delta K_y]$) unstable modes were defined. A schematic representation showing the instability diagram and the location of the selected modes is presented in Figs. 1 and 2 for $k_0 h \to \infty$ and $k_0 h = 1.36$, respectively. The effect of collinear perturbations was also investigated by imposing $\Delta K_y = 0$ (see left panels in Figs. 1 and 2). Note, however, that the resulting lower and upper collinear perturbations have an amplitude that is equivalent to 0.1% of the carrier, i.e. twice the amplitude of an oblique side band. The dimension of the physical domain was defined by a mesh of 256×256 points. The resolution in both dimensions was $\Delta x = \Delta y = 6.24$ m so that the domain includes 10 wavelengths and hence a dominant wave is discretised by 25 grid points. The time step was chosen equal to $\Delta t = T_0/150 = 0.067$ s. On the whole, the simulations estimated the evolution of the surface and velocity potential over a time frame of 350 dominant periods.

4 Temporal evolution of wave amplitude

At each time step, the maximum value of the wave amplitude was estimated from the resulting output surface. A summary of the temporal evolution of the maximum amplitude as normalised by the standard deviation of the wave envelope $E^{1/2}$ is shown in Fig. 3 for different relative depths and steepness. For simplicity only results that were obtained by applying a fifth order expansion (i.e. $M = 5$) in the HOSM are presented in this figure. Wave-wave interactions make the initial surface evolve in time exchanging energy between the carrier wave and the unstable side bands, with the lower disturbances growing faster than the upper ones (see, e.g., Lo and Mei, 1987; Tulin and Waseda, 1999). In a condition of deep water, this energy transfer is followed by a growth of the modulation that leads to a substantial increase of the wave amplitude. This amplification is triggered under the influence of both collinear and oblique disturbances. The process, however, seems to occur more rapidly under the influence of the former (see Fig. 3a, b and c). Interestingly, collinear disturbances also induce a recurrence in the phenomenon with a sequence of modulation and demodulation of the input surface (cf., for example, Ribal et al., 2013). When seeded with oblique side band perturbations, on the other hand, no significant evidence of recurrence can be detected. With the reduction of relative water depth, the region of collinear unstable modes gradually shrinks with a concurrent attenuation of the wave amplitude growth. Eventually, for the critical relative depth $k_0h = 1.36$, collinear modulations become completely stable. As a consequence, energy transfer to collinear side bands no longer occurs (see evolution in time of the wave spectrum in Fig. 4) and concurrently amplitude growth ceases, regardless the value of steepness of the initial surfaces (see dashed line in Fig. 3d, e and f). Oblique modulations, nevertheless, still remains unstable and grow at the expense of the plane wave (see evidence of energy transfer from the plane wave to the oblique side bands in Fig. 5). Note that a first evidence of an energy transfer to oblique side bands can be found in Trulsen et al. (1999), albeit for fairly deep water. In the physical space, the growth of oblique perturbations results in an amplification of the modulation, which roughly doubles its initial amplitude (see solid line in Fig. 3d, e and f). It is also worth mentioning that the time scale for this amplification remains comparable with the one observed in deep water, namely on the order of 100 wave periods. The process speeds up slightly with the increase of the degree of nonlinearity (wave steepness) though.

Despite the fact that the region of instability keeps compressing for further reductions of the relative water depth (see, e.g., Gramstad and Trulsen, 2011), oblique unstable modes still sustain modulational instability and amplitude growth for $k_0h < 1.36$. For the specific case of $k_0h = 1$ (see Fig. 3g, h and i), however, the effect on the modulation attenuates notably. For a low steepness ($k_0 a_0 = 0.1$ for this example), particularly, wave amplitude does not significant depart from the input condition. An increase of steepness seems, however, to reactivate the mechanism, inducing a substantial wave amplification under the influence of oblique disturbances. It is remarkable, in this regard, that the modulation still double its initial amplitude for the largest value of steepness considered in this study (i.e. $k_0 a_0 = 0.14$). This result is in correspondence with simulations of the 2 + 1 NLS (Slunyaev et al., 2002), which demonstrated that rogue waves can still be generated in water of finite depth (i.e. $k_0 h < 1.36$), when a plane wave is seeded by appropriate oblique side bands. In Figs. 6, 7 and 8 the maximum wave amplitude (as normalised by $E^{1/2}$) is presented in function of relative water depth as a summary of the simulation results. On the whole, it is interesting to note that collinear disturbances sustain a substantial amplification of an initially small amplitude modulations (up to twice the initial value) until relatively shallow water conditions with $k_0 h$ as low as 2.4. For $k_0 h \leq 1.36$, amplitude growth ceases completely under the influence of collinear side bands. Oblique perturbations, on the other hand, produces a substantially stronger amplification of the initial modulation already for deep water conditions. In contrast with the behaviour shown by a plane wave seeded with collinear disturbances, the degree of amplification reduces much more gradually, starting from $k_0 h < 48$. Nevertheless, a notable wave amplification still withstands also for $k_0 h \leq 1.36$. It is worth mentioning, however, that the modulation does not grow significantly for relative water depth $k_0 h \leq 0.8$. We remark that results presented so far were obtained using $M = 5$ in the HOSM and hence nonlinear mechanisms other than modulational instability were included. In order to verify whether higher order terms have played a significant role in the observed wave amplification in water of finite depth, it is instructive to compare the simulations with runs that were performed with $M = 3$, where only four-waves interactions were included. This comparison is presented for both cases of collinear and oblique disturbances in Fig. 9.

Despite some differences, higher order terms does not seems to produce any substantial variation in the results. This seems to corroborate that four waves interaction

NHESSD

1, 5237–5260, 2013

Rogue waves in finite water depth

L. Fernandez et al.

and hence modulational instability dominates the nonlinear dynamics of the wave fields also in water of finite depth with relative depth $k_0h < 1.36$, provided the carrier wave is seeded by appropriate oblique side band perturbations.

5 Conclusions

Direct numerical simulations of the Euler equations using the Higher Order Spectral Method introduced by (West et al., 1987) were used to investigate the nonlinear wave dynamics in finite water depth. Particularly, simulations were undertaken to investigate the role of oblique unstable perturbations in withstanding modulational instability beyond the critical relative water depth $k_0h = 1.36$. Simulations were carried out by tracking the temporal evolution of an initial surface composed by a plane wave and four oblique side band perturbations carefully selected within the region of instability. The physical domain was defined to include 10 dominant wavelengths and discretised with 256×256 grid points. A time step corresponding to $T_0/150$ was imposed, where T_0 is the period of the carrier wave. Runs were performed for different combinations of wave steepness and water depth so that a wide range of relative depth here defined and ranging from deep to shallow water conditions ($0.5 < k_0h < \infty$). Configurations using collinear perturbations were also applied for comparison. As expected, results indicated that modulational instability ceases quite suddenly at $k_0h = 1.36$, when the plane wave is seeded with collinear perturbations in agreement with Benjamin (1967) and Janssen and Onorato (2007). Under the influence of unstable side bands, however, modulational instability survives beyond this critical water depth and a substantial amplification of wave amplitude is observed until relative water depth $k_0h = 0.8$. Beyond this threshold, simulations did not indicate any significant growing of the modulations, though.

Acknowledgements. F. W. O. project G.0333.09 and EU project EXTREME SEAS (contract SCP8-GA-2009-234175) are acknowledged. The authors also acknowledge the Hercules Foun-

dation and the Flemish Government department EWI for providing access to the Flemish Supercomputer Center.

References

Annenkov, S. Y. and Shrira, V. I.: Numerical modeling of water–wave evolution based on the Zakharov equation, J. Fluid. Mech., 449, 341–371, 2001. 5243

Babanin, A. V., Waseda, T., Kinoshita, T., and Toffoli, A.: Wave breaking in directional fields, J. Phys. Oceanogr., 41, 145–156, 2011. 5238, 5239

Bailung, H., Sharma, S. K., and Nakamura, Y.: Observation of Peregrine Solitons in a Multicomponent Plasma with Negative Ions, Phys. Rev. Lett., 107, 255005, doi:10.1103/PhysRevLett.107.255005, 2011. 5238

Benjamin, T. B.: Instability of periodic wave trains in nonlinear dispersive systems, Proc. Roy. Soc. London, A299, 59–75, 1967. 5239, 5247

Benjamin, T. B. and Feir, J. E.: The disintegration of wave trains on deep water. Part I. Theory, J. Fluid Mech., 27, 417–430, 1967. 5238

Benney, D. J. and Roskes, G. J.: Wave instabilities, Stud. Appl. Math, 48, 377–385, 1969. 5239

Bitner-Gregersen, E. M. and Toffoli, A.: On the probability of occurrence of rogue waves, Natural Hazards and Earth System Science, 12, 751–762, 2012. 5238

Chabchoub, A., Hoffmann, N., and Akhmediev, N.: Rogue wave observation in a water wave tank, Physical Review Letters, 106, 204502, doi:10.1103/PhysRevLett.106.204502, 2011. 5238

Chalikov, D.: Freak waves: Their occurrence and probability, Physics of Fluids, 21, 1–4, 2009. 5238

Clamond, D. and Grue, J.: A fast method for fully nonlinear water–wave computations, J. Fluid Mech., 447, 337–355, 2001. 5243

Clamond, D., Francius, M., Grue, J., and Kharif, C.: Long time interaction of envelope solitons and freak wave formations, Europ. J. Mech. B/Fluids, 25, 536–553, 2006. 5243

Dean, R. and Dalrymple, R.: Water Wave Mechanics for Engineers and Scientists, Advanced Series on Ocean Engineering – vol. 2, World Scientific Pub. Co., Singapore, reprint, 2000. 5242

Dommermuth, D. G. and Yue, D. K.: A high–order spectral method for the study of nonlinear gravity waves, J. Fluid Mech., 184, 267–288, 1987. 5240

Ducrozet, G., Bonnefoy, D., Le Touzé, D., and Ferrant, P.: 3-D HOS simulations of extreme waves in open seas, Nat. Hazards Earth Syst. Sci., 7, 109–122, 2007, http://www.nat-hazards-earth-syst-sci.net/7/109/2007/. 5243

Francius, M. and Kharif, C.: Three dimensional instabilities of periodic gravity waves in shallow water, J. Fluid Mech., 561, 417–437, 2006. 5243

Gramstad, O. and Trulsen, K.: Hamiltonian form of the modified nonlinear Schrödinger equation for gravity waves on arbitrary depth, J. Fluid Mech., 670, 404–426, 2011. 5239, 5245

Janssen, P. A. E. M. and Onorato, M.: The intermediate water depth limit of the Zakharov equation and consequences for wave prediction, J. Phys. Oceanogr., 37, 2389–2400, 2007. 5239, 5247

Kharif, C., Pelinovsky, E., and Slunyaev, A.: Rogue Waves in the Ocean, Advances in Geophysical and Environmental Mechanics and Mathematics, Springer, Berlin, 2009. 5238

Kibler, B., Fatome, J., Finot, C., Millot, G., Dias, F., Genty, G., Akhmediev, N., and Dudley, J.: The Peregrine soliton in nonlinear fibre optics, Nature Physics, 6, 790–795, 2010. 5238

Kristiansen, O., Fructus, D., Clamond, D., and Grue, J.: Simulations of crescent water wave patterns on finite depth, Phys. Fluids, 17, 064101, doi:10.1063/1.1920351, 2005. 5243

Lo, E. Y. and Mei, C. C.: Slow evolution of nonlinear deep-water waves in 2 horizontal directions – a numerical study, Wave Motion, 9, 245–259, 1987. 5245

McLean, J. W.: Instabilities of finite-amplitude gravity waves on water of finite depth, J. Fluid Mech., 114, 331–341, 1982. 5239, 5243

Mori, N. and Yasuda, T.: Effects of high–order nonlinear interactions on unidirectional wave trains, Ocean Engineering, 29, 1233–1245, 2002. 5243

Onorato, M., Proment, D., Clauss, G., and Klein, M.: Rogue Waves: From Nonlinear Schrödinger Breather Solutions to Sea-Keeping Test, PloS one, 8, e54629, doi:10.1371/journal.pone.0054629, 2013a. 5238

Onorato, M., Residori, S., Bortolozzo, U., Montina, A., and Arecchi, F. T.: Rogue waves and their generating mechanisms in different physical contexts, Physics Reports, 528, 47–89, 2013b. 5238

Osborne, A., Onorato, M., and Serio, M.: The nonlinear dynamics of rogue waves and holes in deep–water gravity wave train, Phys. Lett. A, 275, 386–393, 2000. 5239

Osborne, A. R.: Nonlinear Ocean Waves and the Inverse Scattering Transform, International Geophysics Series, Elsevier, San Diego, 2010. 5238, 5239
Ribal, A., Babanin, A. V., Young, I., Toffoli, A., and Stiassnie, M.: Recurrent solutions of the Alber equation initialized by Joint North Sea Wave Project spectra, J. Fluid Mech., 719, 314–344, 2013. 5239, 5245
Slunyaev, A., Kharif, C., Pelinovsky, E., and Talipova, T.: Nonlinear wave focusing on water of finite depth, Physica D, 173, 77–96, 2002. 5239, 5240, 5246
Solli, D. R., Ropers, C., Koonath, P., and Jalali, B.: Optical rogue waves, Nature, 450, 1054–1057, 2007. 5238
Tanaka, M.: A method of studying nonlinear random field of surface gravity waves by direct numerical simulations, Fluid Dynam. Res., 28, 41–60, 2001a. 5242, 5243
Tanaka, M.: Verification of Hasselmann's energy transfer among surface gravity waves by direct numerical simulations of primitive equations, J. Fluid Mech., 444, 199–221, 2001b. 5242, 5243
Toffoli, A., Bitner-Gregersen, E., Onorato, M., and Babanin, A. V.: Wave crest and trough distributions in a broad–banded directional wave field, Ocean Engineering, 35, 1784–1792, 2008a. 5243
Toffoli, A., Onorato, M., Bitner-Gregersen, E., Osborne, A. R., and Babanin, A. V.: Surface gravity waves from direct numerical simulations of the Euler equations: a comparison with second–order theory, Ocean Engineering, 35, 367–379, 2008b. 5238, 5243
Toffoli, A., Benoit, M., Onorato, M., and Bitner-Gregersen, E. M.: The effect of third-order nonlinearity on statistical properties of random directional waves in finite depth, Nonlin. Processes Geophys., 16, 131–139, 2009, http://www.nonlin-processes-geophys.net/16/131/2009/. 5240, 5243
Toffoli, A., Gramstad, O., Trulsen, K., Monbaliu, J., Bitner-Gregersen, E. M., and Onorato, M.: Evolution of weakly nonlinear random directional waves: laboratory experiments and numerical simulations, J. Fluid Mech., 664, 313–336, 2010. 5243
Trulsen, K. and Dysthe, K. B.: A modified nonlinear Schrödinger equation for broader bandwidth gravity waves on deep water, Wave Motion, 24, 281–289, 1996. 5239
Trulsen, K., Stansberg, C. T., and Velarde, M. G.: Laboratory evidence of three-dimensional frequency downshift of waves in a long tank, Phys. Fluids, 11, 235, 1999. 5239, 5245
Tulin, M. P. and Waseda, T.: Laboratory observation of wave group evolution, including breaking effects, J. Fluid Mech., 378, 197–232, 1999. 5245

West, B. J., Brueckner, K. A., Jand, R. S., Milder, D. M., and Milton, R. L.: A new method for surface hydrodynamics, J. Geophys. Res., 92, 11803–11824, 1987. 5240, 5242, 5243, 5247

Whitham, G.: Linear and Nonlinear Waves, Wiley Interscience, New York, 1974. 5239

Xiao, W., Liu, Y., Wu, G., and Yue, D. K. P.: Rogue wave occurrence and dynamics by direct simulations of nonlinear wave-field evolution, J. Fluid Mech., 720, 357–392, 2013. 5243

Zakharov, V.: Stability of period waves of finite amplitude on surface of a deep fluid, J. Appl. Mech. Tech. Phys., 9, 190–194, 1968. 5238, 5241

Zakharov, V. and Ostrovsky, L.: Modulation instability: The beginning, Physica D: Nonlinear Phenomena, 238, 540–548, 2009. 5238

Zakharov, V. E., Dyachenko, A. I., and Vasilyev, O. A.: New method for numerical simulation of a nonstationary potential flow of incompressible fluid with a free surface, Europ. J. Mech. B/Fluids, 21, 283–291, 2002. 5243

NHESSD

1, 5237–5260, 2013

Rogue waves in finite water depth

L. Fernandez et al.

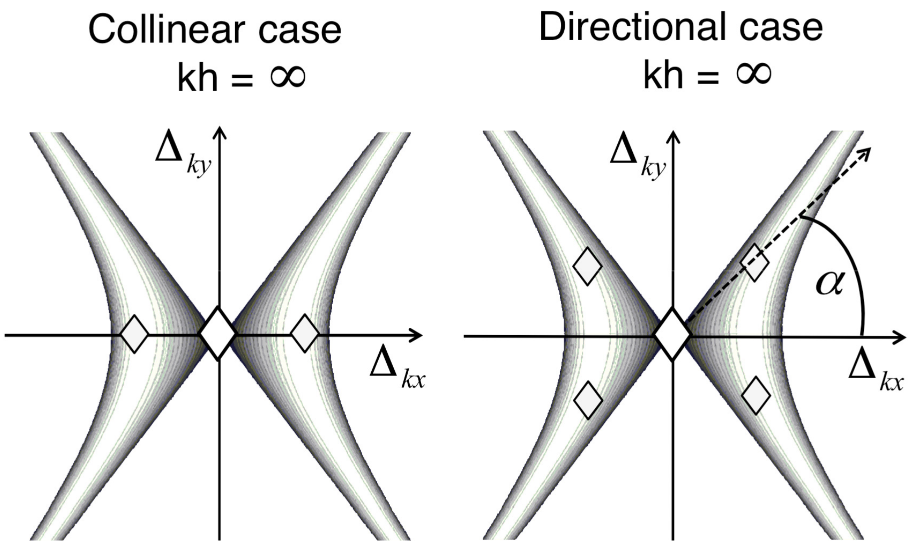

Fig. 1. Instability region and location of side bands for $k_0 h \rightarrow \infty$: collinear disturbances (left panel); oblique disturbances (right panel).

NHESSD
1, 5237–5260, 2013

Title Page
Abstract Introduction
Conclusions References
Tables Figures
◀I ▶I
◀ ▶
Back Close
Full Screen / Esc
Printer-friendly Version
Interactive Discussion

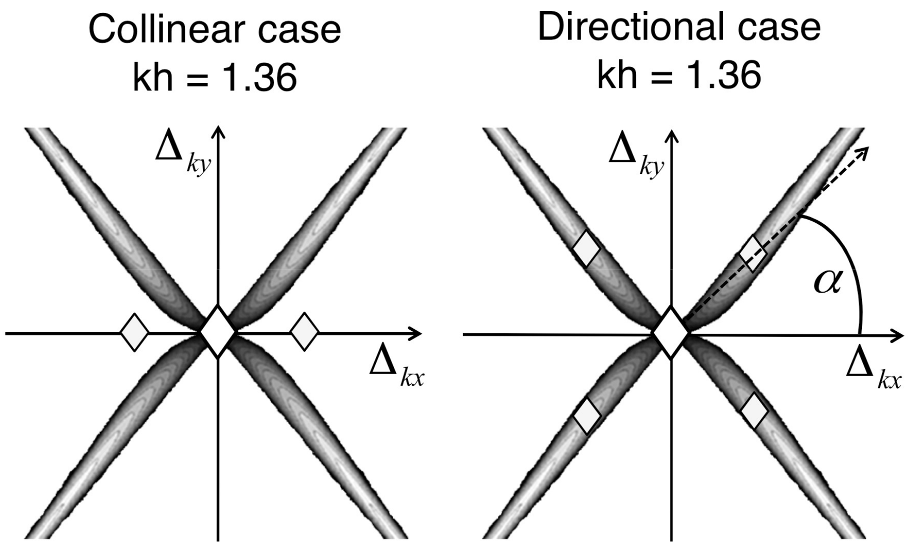

Fig. 2. Instability region and location of side bands for $k_0h = 1.36$: collinear disturbances (left panel); oblique disturbances (right panel).

NHESSD
1, 5237–5260, 2013

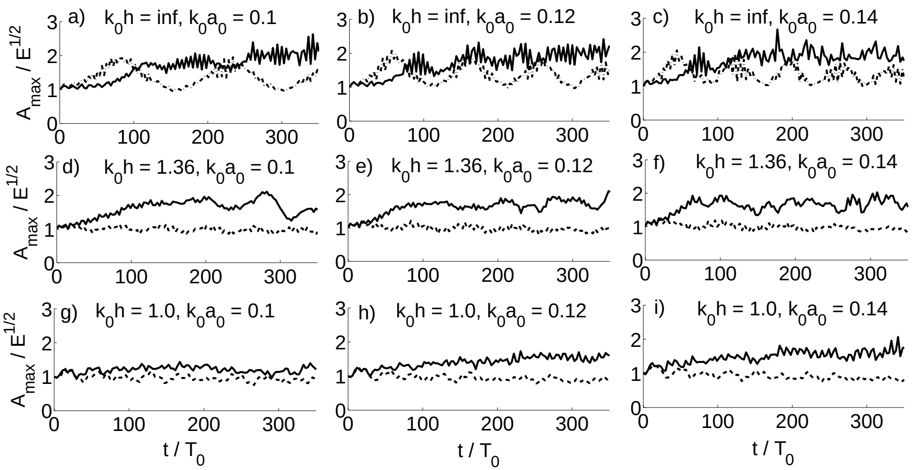

Fig. 3. Evolution in time of the normalised maximum amplitude: plane wave seeded with collinear perturbations (dashed line); plane wave seeded with oblique perturbations (solid line).

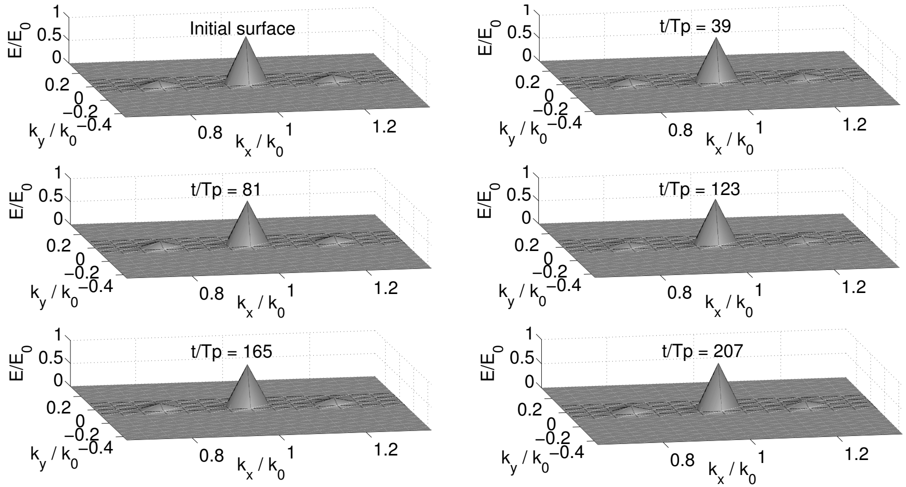

Fig. 4. Wave number spectrum evolution in time. Case: plane wave with collinear perturbations in relative water depth $kh = 1.36$.

NHESSD
1, 5237–5260, 2013

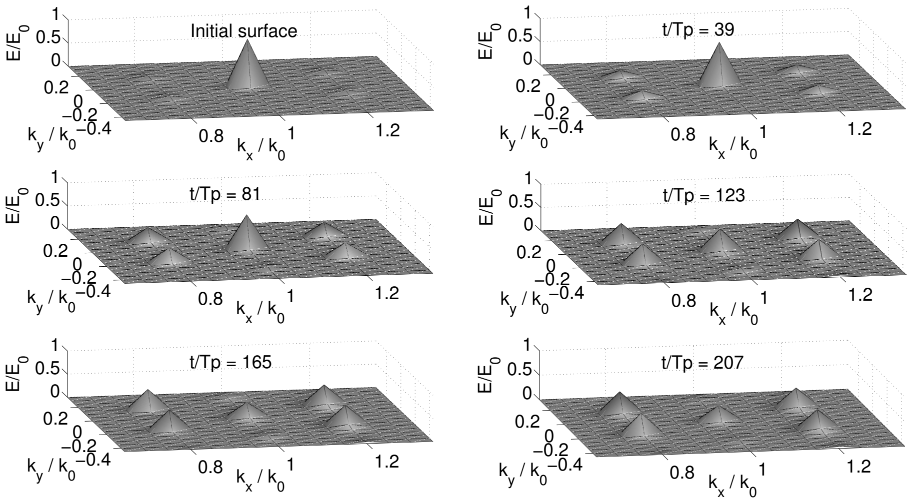

Fig. 5. Wave number spectrum evolution in time. Case: plane wave seeded with oblique perturbations in relative water depth $kh = 1.36$.

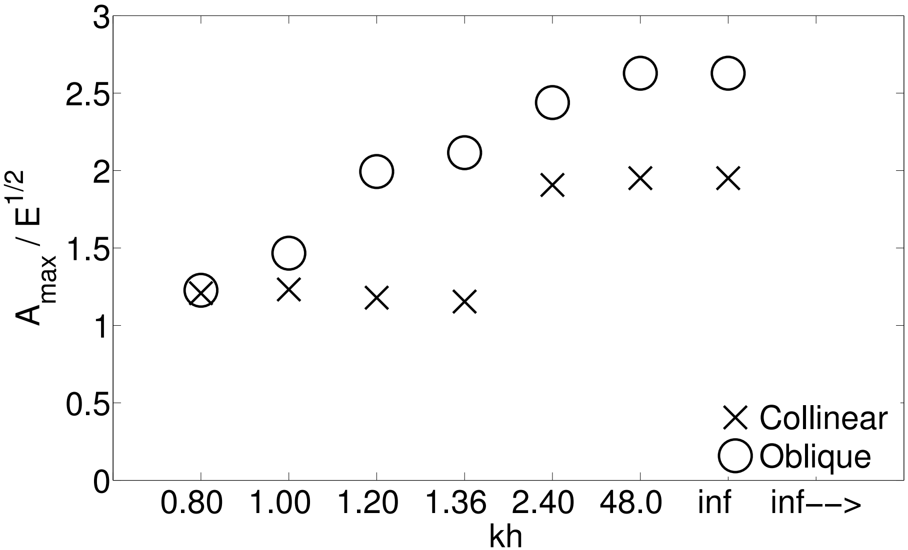

Fig. 6. Maximum wave amplification in function of *kh* for $k_0 a_0 = 0.1$, $M = 5$.

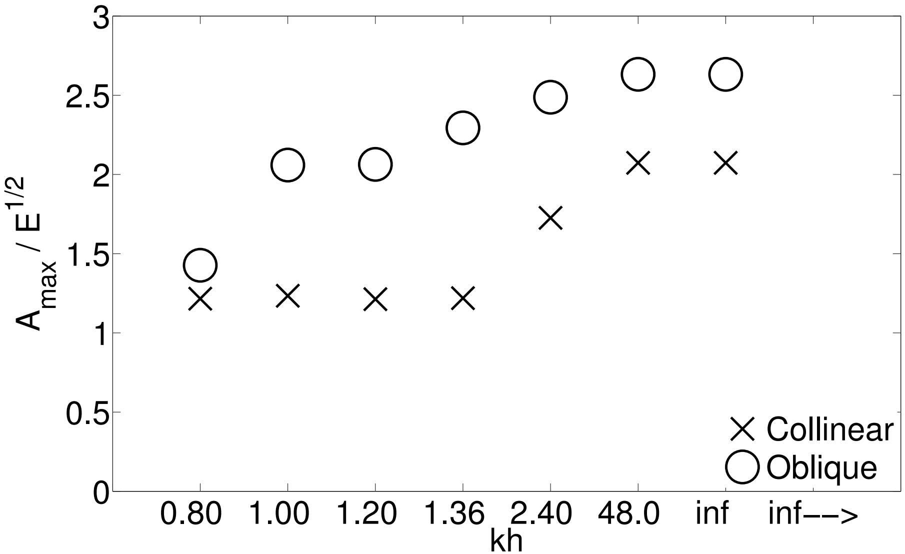

Fig. 7. Maximum wave amplification in function of kh for $k_0 a_0 = 0.12$, $M = 5$.

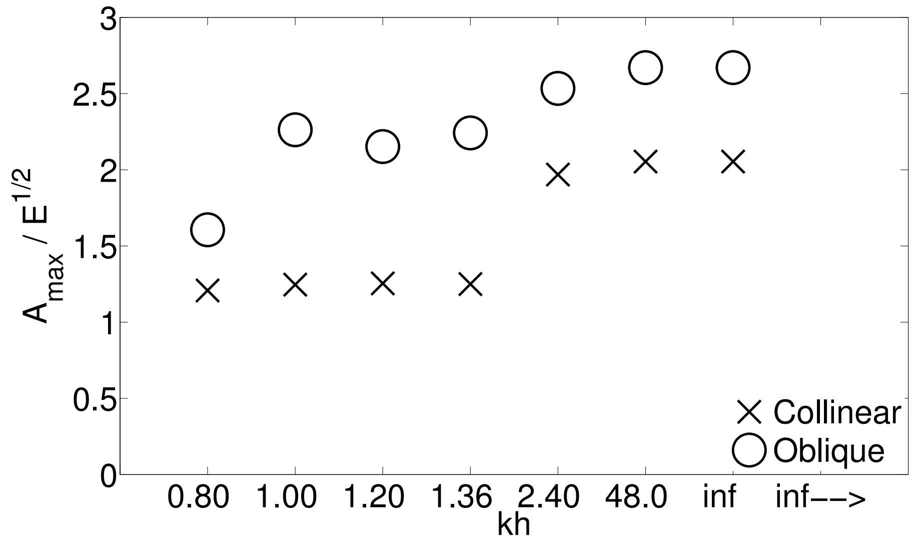

Fig. 8. Maximum wave amplification in function of *kh* for $k_0 a_0 = 0.14$, $M = 5$.

NHESSD
1, 5237–5260, 2013

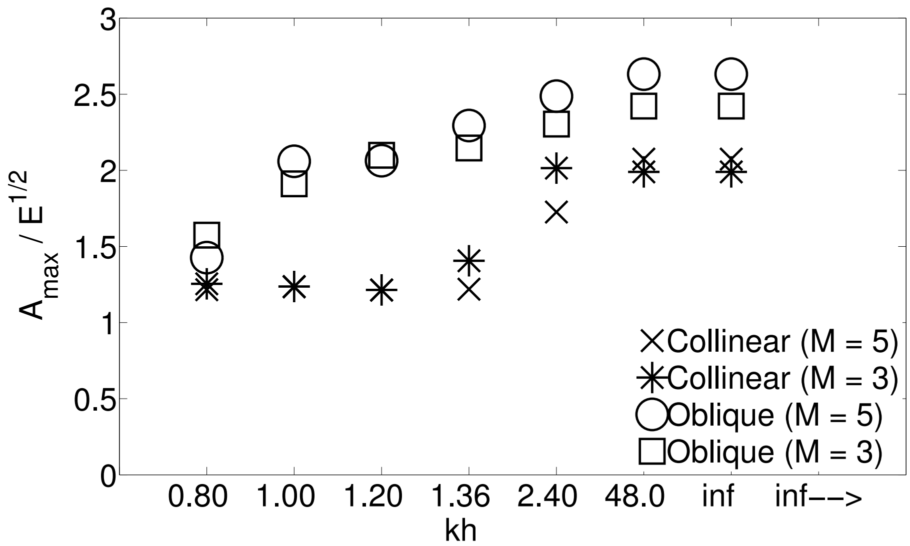

Fig. 9. Comparison with different orders.

NHESSD
1, 5237–5260, 2013